DYNA
http://dyna.medellin.unal.edu.co/

UNIVERSIDAD NACIONAL DE COLOMBIA

The empirical correlation between shear wave velocity and penetration resistance for the eolian sand deposits in the city of Olmos-Peru

Cristhian Gerardo Alhuay-León [a] & Pablo Cesar Trejo-Noreña [b]

[a] *Department of Civil Engineering, National University of Engineering, Lima, Peru. calhuayl@uni.pe*
[b] *Posgraduate Department of Civil Engineering, National University of Engineering, Lima, Peru. ptrejon@uni.edu.pe*

Received: February 2nd, 2021. Received in revised form: April 20th, 2021. Accepted: April 30th, 2021.

Abstract
Shear wave velocities (Vs) and the number of blows of SPT (N) are parameters that are generally recorded in a geotechnical exploration campaign, in the literature there are several publications on the empirical correlations between N y Vs in different types of soil, the first studies being attributed to Japanese researchers in the 60s and 70s. North Peruvian pipeline was built on a recent quaternary eolian deposit, so a research area in Olmos near to the structure was used for tests. In the geotechnical research campaign were carried out in an arrangement multi-channel and standard penetration test in order to obtain Vs and N respectively. The correlations in this publication are for eolian sand deposits that can potentially be used in other regions with similar characteristics. The correlations presented are; N_{60} - Vs considering and incorporating into the model the influence of the effective overload.

Keywords: shear wave velocity; standard penetration test; eolian sand.

Correlación empírica entre velocidades de ondas de corte y el número de golpes del SPT en depósitos de arenas eólicas de la ciudad de Olmos-Perú

Resumen
Las velocidades de ondas de corte (Vs) y el número de golpes de SPT (N) son parámetros que generalmente se registran en una campaña de exploración geotécnica, en la literatura existen diversas publicaciones sobre correlaciones empíricas entre N y Vs en distintos tipos de suelo, siendo los primeros estudios atribuido a investigadores japoneses en la década de los 60 y 70. El oleoducto norperuano fue construido sobre un depósito eólico del cuaternario reciente, por lo que se utilizó un área de investigación en Olmos cerca de la estructura para los ensayos. En la campaña de investigaciones geotécnicas se realizaron ensayos de medición de ondas superficiales en arreglo multicanal y ensayos de penetración estándar con la finalidad de obtener Vs y N respectivamente. Las correlaciones en esta publicación son para depósitos de arenas eólicas que pueden ser utilizadas potencialmente en otras regiones de similares características. Se presenta las correlaciones; N_{60} – Vs considerando e incorporando al modelo la influencia de la sobrecarga efectiva.

Palabras clave: velocidad de ondas de corte; ensayo de penetración estándar; arena eólica.

1. Introduction

The North Peruvian Pipeline is one of the most important works in the last years. This pipeline has three branches which are the following: Branch I, branch II and ORN. In branch II, the pipeline passes through areas in the Lambayeque's region. Geological and geotechnical similar conditions were found in an area close to the structure. This area is located in the New City of Olmos, the district of Olmos (Fig.1). This city is a project that proposes a planned

How to cite: Alhuay-León, C.G. and Trejo-Noreña, P.C., The empirical correlation between shear wave velocity and penetration resistance for the eolian sand deposits in the city of Olmos-Peru.. DYNA, 88(217), pp. 247-255, April - June, 2021.

and self-sustaining city with modern urban criteria, located in the north of the Peruvian coast where eolian deposits lie in its entirety.

In the geotechnical exploration campaign of the project, a series of in situ tests were carried out, from which standard penetration tests (SPT) and Multichannel Surface Wave Analysis measurement (MASW) were selected in order to compare their respective records and determine an empirical correlation equation for eolian sand deposits.

In geotechnical practice, it is known that the SPT is widely accepted in different countries and has a large amount of database and correlations due to its wide use in geotechnics. On the other hand, the MASW test is a geophysical method with which a profile of shear wave velocities (Vs) is obtained, from the dispersive nature of the surface waves of soil [1-3] and whose typical field application were originally proposed by [3]. The profile of shear wave velocities is fundamental for the characterization of a site and the evaluation of its dynamic response [4].

The N versus Vs database is correlated and fitted to a potential function of the form $V_S = AN^B$, where A and B are obtained from a statistical technique of linear regression analysis to model the relationship between variables [5]. The correlations presented in this publication are: N_{60} - V_S (N corrected to 60% energy) and N_{60} - V_S introducing the influence of the effective overload in the model.

Consequently, the proposed correlation may be used in eolian areas, which generally occur in large areas of the Peruvian coast. Although it is preferable to determine N of SPT directly from in situ tests, there are often difficulties with respect to the execution time and cost of the test by its very nature, therefore it is a considerable advantage to propose a correlation methodology that allows a preliminary estimate of the value of N of SPT or vice versa, since they are a very important data for the mechanical characterization of the site.

2. Study area and geological aspects

2.1 Study area

The study area is located in the district of Olmos, province and department of Lambayeque, Peru. The "La Nueva Ciudad de Olmos" project was developed in a program created by the Ministry of Housing, Construction and Sanitation, with the aim of creating a planned and self-sustaining city with modern urban planning criteria, to be replicated in new processes of urbanization in Peru.

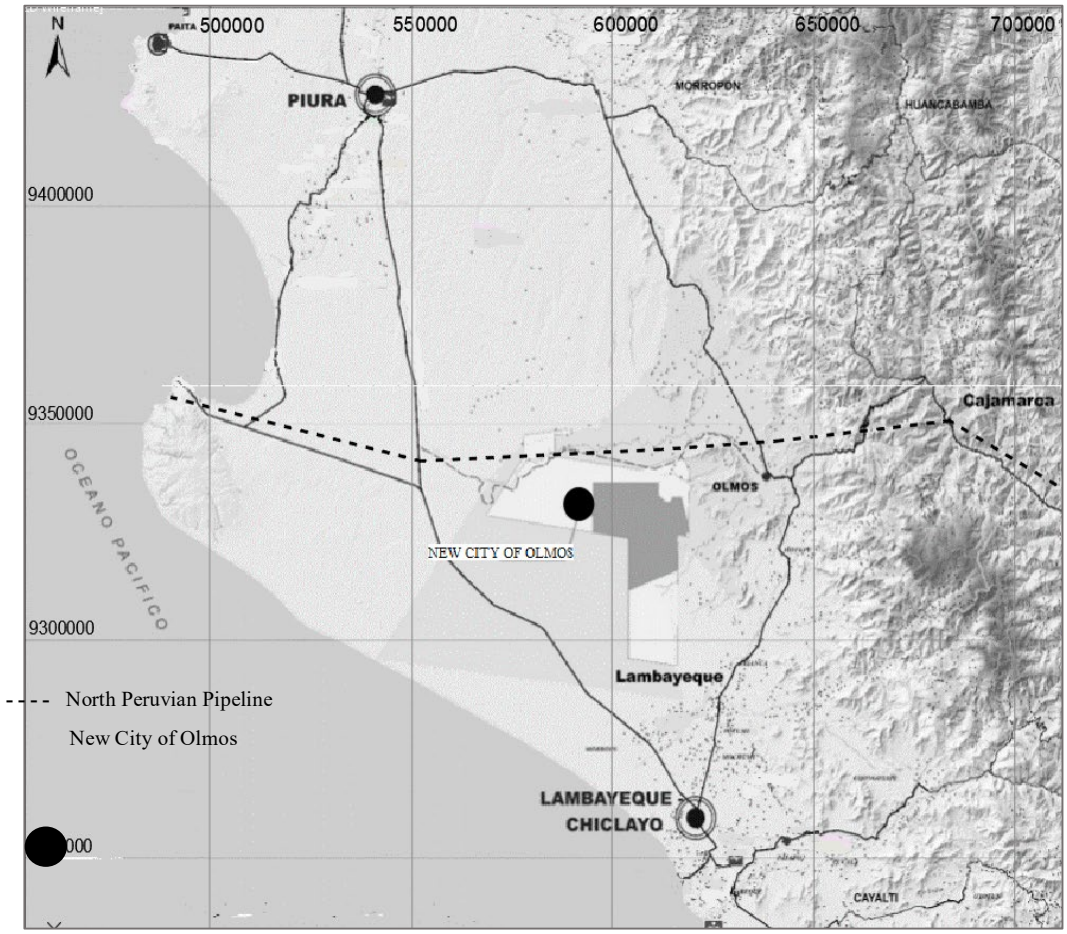

Figure 1. Location of the study area
Source: The authors

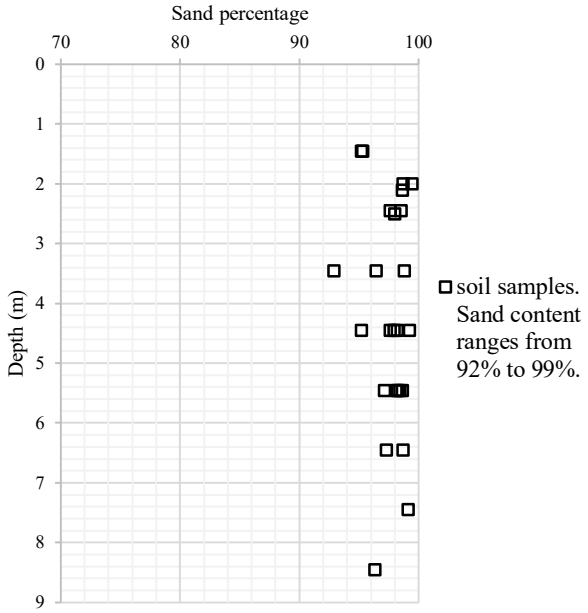

Figure. Summary of soil classification tests (SUCS).
Source: The authors.

2.2 Geology of the study area

From the geological point of view, the study area is located on the eolian deposit recent of quaternary (Qr-e), as observed in the Geological Map of the Quadrangle of Las Salinas 13-c, elaborated by [6] at the Geological, Mining and Metallurgical Institute (INGEMMET), as shown in Fig. 3.

The Qr-2 deposit is composed by poorly graded sands of fine grain (Fig. 2), from loose to moderately dense compactness, in a dry state, reaching depths of 4.0 to 9.0 m according to SPT records. The Vs velocities in this deposit are generally less than 280 m/s. No phreatic level is recorded.

The Pleistocene eolian deposit (Qp-e) is underlying the Qr-e deposit, and is made up of poorly graded sand of medium grain and silty sand, of dense compactness, and the Vs velocities are generally greater than 280 m/s.

In the Seismic Zoning Map of Peru, the study area is located in the zone of greatest seismic activity, with a maximum horizontal acceleration of 0.45g in rigid soil with a probability of 10% of being exceeded in 50 years [7]. In the study area, the Vs30 is in the range of 180 to 360 m/s corresponding to Type D soil "Rigid Soil", according to the classification based on the National Earthquake Reduction Program (NEHRP).

3. Empirical correlation between N of SPT and Vs

In the literature there is a record of numerous correlations between N of SPT and the VS speeds for different types of soil, finding that these vary significantly even for the same type of soil.

Most correlations incorporate N and Vs obtained directly from the field, and some correct the value of N at 60% of energy, such as [8-12]; On the other hand, few correlations introduce the correction for effective overload to N and Vs, as the works of [11-13], among others, who introduce this correction, through a multiple linear regression analysis. [14] recently established a unified empirical correlation between Vs and N that depend on effective confining stress, fines content, and plasticity index through the conditional prediction approach, for a wide range of soil types.

Table 1 shows the compilation of some correlations in sands, based on Vs-N (N and Vs without correction) and Vs-N_{60}. The first studies are attributed to japanese researchers between the 60s and 70s: [15-18], among others.

Table 1.
Some correlations collected between Vs and N in sands.

Authors	N - Vs (without correction)	Vs - N_{60}
[16]	$V_S = 31.7\ N^{0.5}$	-
[19]	$V_S = 87\ N^{0.36}$	-
[18]	$V_S = 59.4\ N^{0.47}$	-
[20]	$V_S = 80.6\ N^{0.331}$	-
[21]	$V_S = 98.3\ N^{0.25}$	-
[22]	$V_S = 87.8\ N^{0.29}$	-
[23]	$V_S = 100.6\ N^{0.29}$	-
[24]	$V_S = 57.4\ N^{0.49}$	-
[8]	-	$V_S = 88.4\ (N_{60}+1)^{0.29}$
[25]	$V_S = 123.4\ N^{0.29}$ $V_S = 100\ N^{0.24}$	--
[9]	-	$V_S = 145\ N_{60}^{0.178}$
[26]	$V_S = 90.82\ N^{0.319}$	$V_S = 131\ N_{60}^{0.205}$
[27]	$V_S = 79\ N^{0.434}$	-
[28]	$V_S = 73\ N^{0.33}$	-
[11]	-	$V_S = 124.1\ N_{60}^{0.216}$
[12]	$V_S = 100.53\ N^{0.265}$	$V_S = 96.29\ N_{60}^{0.266}$
[29]	$V_S = 60.17\ N^{0.56}$	-
[30]	$V_S = 107\ N^{0.34}$	-
[31]	$V_S = 77\ N^{0.355}$	-
[32]	$V_S = 100.3\ N^{0.338}$	-

Source: The authors.

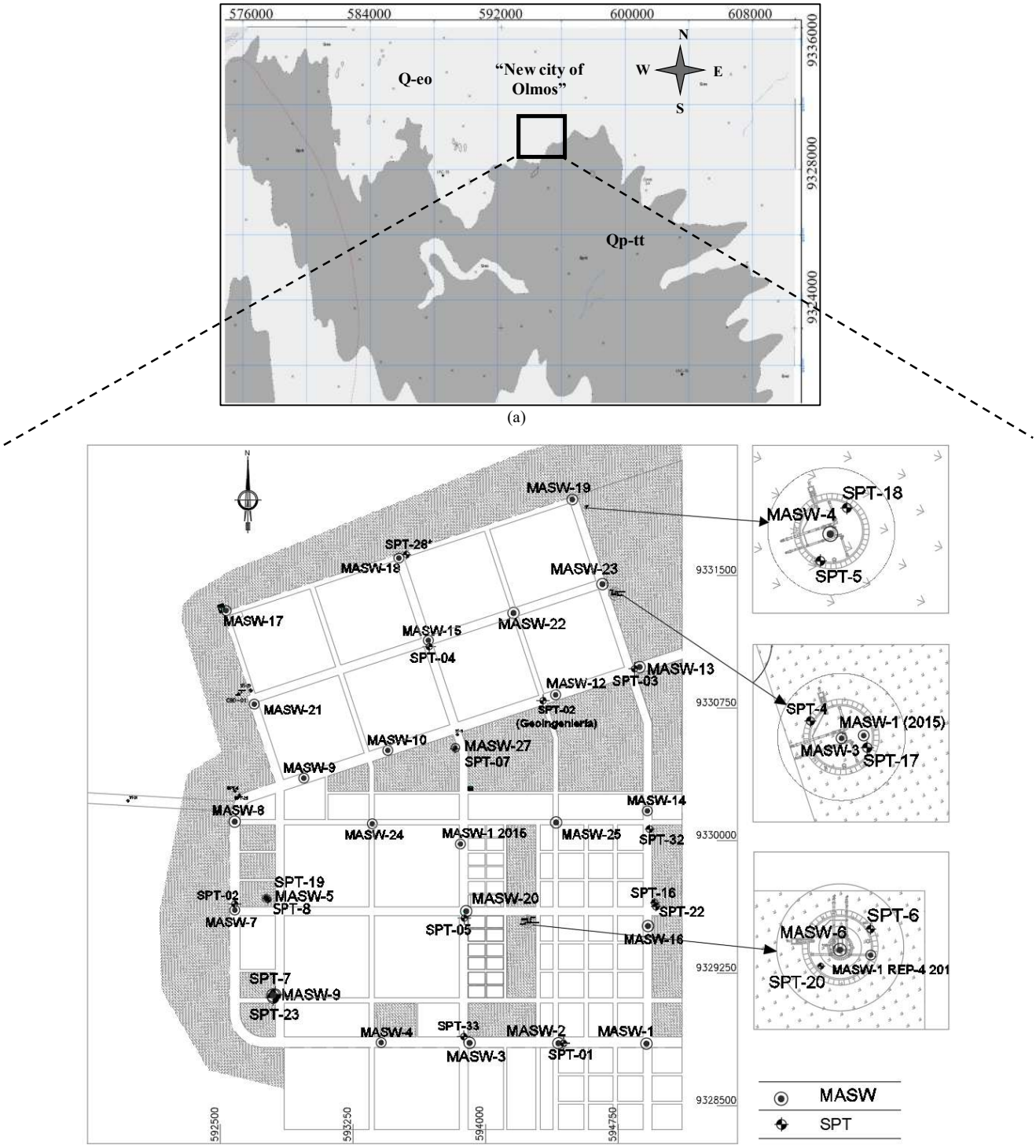

Figure 3. (a) Geological map of the Las Salinas 13c. (b) Location map of the SPT y MASW test.
Source: The authors.

3.1 Data collection

SPT remains the most current test for geotechnical site characterization. The test is simple and provides a sample of disturbed soil while measuring resistance to penetration [33]. Fig. 4 presents the compilation of the SPT tests, these present a record up to a depth of 7.00 to 12.0 m, generally the number of SPT blows is less than 30, corresponding to poorly graded sands of loose compactness to moderately dense. Some SPT tests reach a number of blows greater than 30, corresponding to the dense compact sand layer and associated with the ancient Pleistocene eolian deposit.

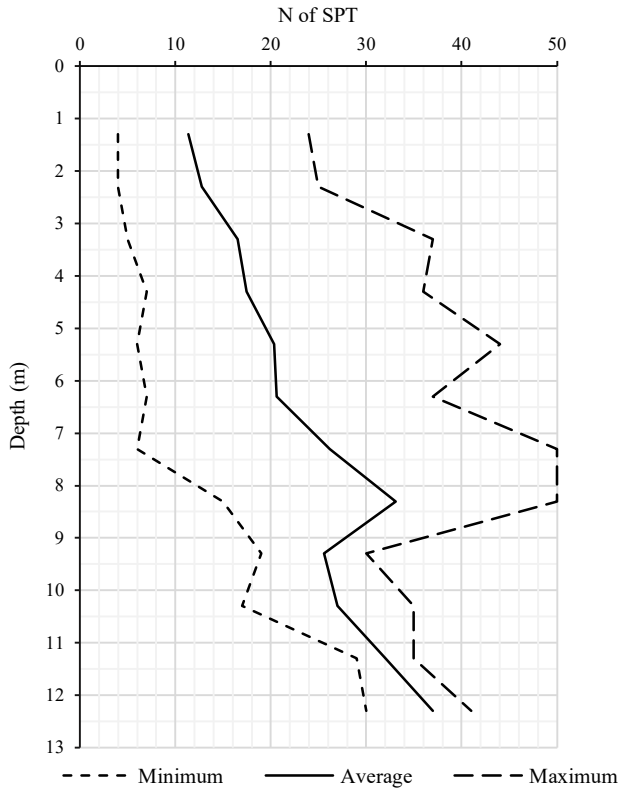

Figure 4. SPT test report.
Source: The authors.

To standardize the number of SPT blows at 60% of hammer energy and other correction factors, the SPT test equipment and procedure was considered. Eq. (1) incorporates these corrections:

$$N_{60} = \frac{N \; Er \; C_B \; C_R \; C_S}{60\%} \quad (1)$$

N: Number of blows of SPT
Er: Energy relation of the hammer.
CB: Correction factor for well diameter.
CR: Correction factor for rod length.
CS: Correction factor for use of standard sampler or sampler without liners.

In this study, it was considered to use an energy ratio (Er) of 70%, to estimate this value the mechanism of execution of the tests was considered; the use of a 63.5 kg Donut hammer, 76 cm fall height and 2 turns of rope on the cathead, under the same mechanism [34] propose an Er of 75%, on the other hand, [35] experimentally measured the hammer fall speed for 2 and 3 turns of rope to the cathead obtaining an Er of 69% and 42% respectively, in a test well of poorly graded sand. [36] obtained an average energy ratio of 70.5%.

The drilling diameter is 2.5" [37] proposes a correction CB=1.

No liners in the sample were used in the split cane, therefore, the correction factor is considered Cs = 1.2, according to the proposal by [37, 38].

The correction factor for rod length is followed as suggested in Table 2.

Table 2.
Correction for rod length.

Length	Value
Length <3.0m	0.75
Length 3-4	0.80
Length 4-6	0.85
Length 6-10	0.90
Length 10-30	1.00

Source: The authors.

The acquisition of data from the MASW tests was carried out using a Geometrics brand 24-channel Geode Seismograph. The test scheme consists of a linear arrangement of 24 vertical geophones of 4.5 Hz frequency. The source of seismic waves is the impact of a 25-pound (11.3 kg) hammer on a metal plate.

The generation of a dispersion curve is one of the most critical steps to finally generate a profile of shear wave velocities [3]. Given the in-situ conditions, the generation of the scattering image has good quality as shown in Fig. 5, where the scattering curve in the fundamental mode can be identified quite clearly.

The quality of the scattering image is due to the favorable conditions that the study area presents for data acquisition, for example; The little or almost no external noise during data acquisition made it possible to efficiently obtain records even with a single hammer blow, on the other hand, the study area presents a slight topographic variation of less than 10º. [40] point out that the dispersion characteristic can be estimated with less than 4% of error when the topographic slope along the line is less than 10º.

Constructing the scattering image and extracting the signal scattering curve is carried out through the phase shift method (also known as the wavefield transformation method), which was first described by [41].

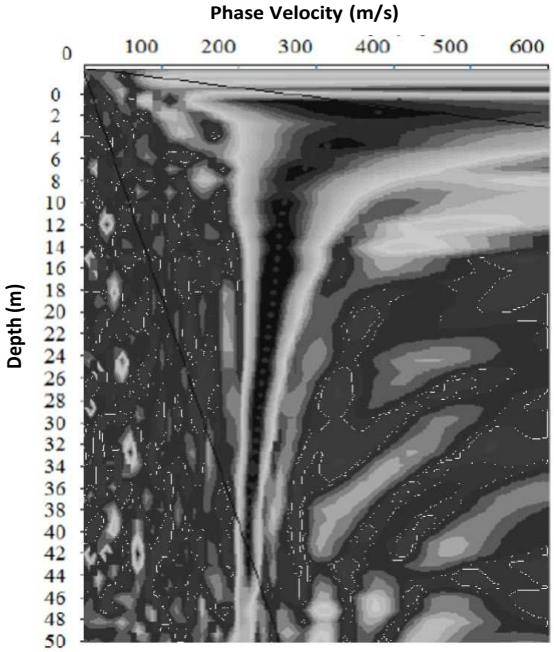

Figure 5. Dispersion image quality.
Source: The authors.

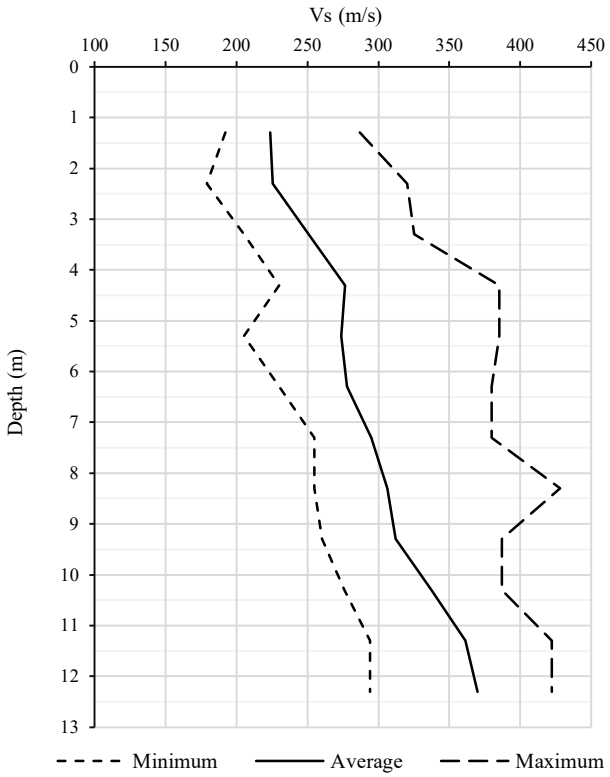

Figure 6. Shear wave velocity profile.
Source: The authors.

MASW tests generally reached depths of up to 30 m. Fig. 6 shows Vs velocity records down to depths from 7.0 to 12.0 for comparative purposes with the SPT tests.

3.2 The correlation equation

The potential equation ($Vs = A.N^B$) expressed in natural logarithms results in a linear equation Eq. (2) of the form:

$$\ln V_S = \ln A + B \ln N + \varepsilon \quad (2)$$

The natural logarithm of A y el parameter B are obtained with a simple linear regression analysis. The correlation equations obtained are Eq. (3, 4):

$$V_S = 142.59\ N^{0.222} \quad (3)$$

N and Vs obtained from field

$$V_S = 141.14\ (N_{60})^{0.212} \quad (4)$$

The N of SPT and Vs obtained directly from the field and the correlations in sands (without correction of N and Vs) of some authors are presented in Fig. 7 and it is observed that the curves vary among themselves, probably because N does not present correction and is dependent on the variability of the equipment and SPT test procedure. The correlation in this study is $V_S = 142.59\ N^{0.222}$, and it generously approximates the curves of [30,32].

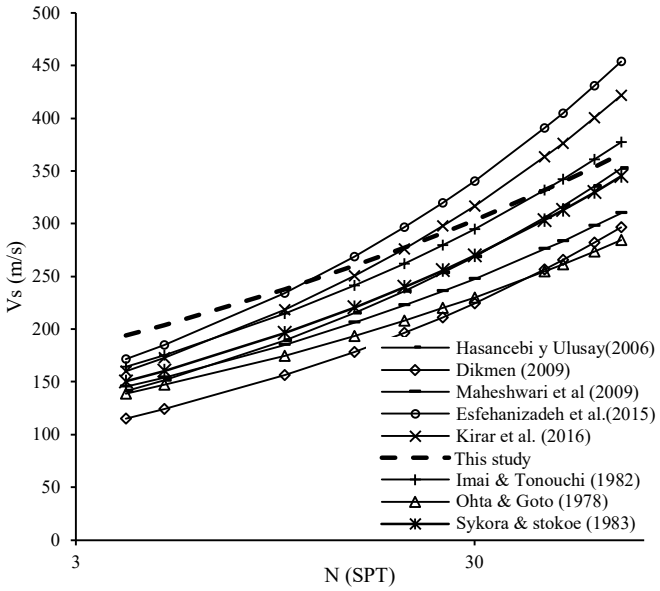

Figure 7. Correlation of N – Vs (N y Vs Uncorrected).
Source: The authors.

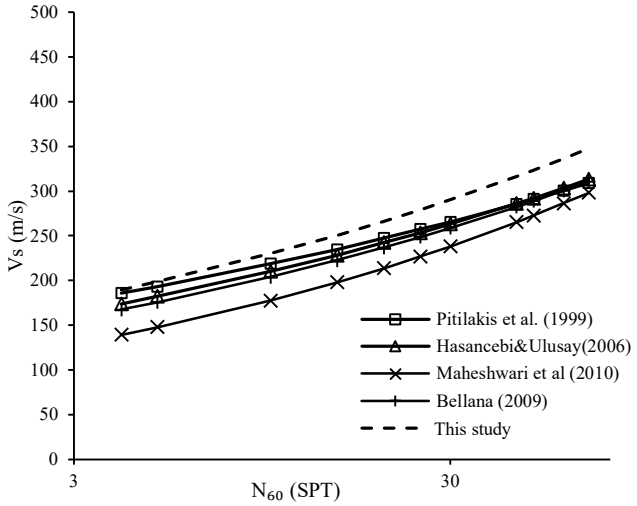

Figure 8. Correlation of N_{60} – Vs.
Source: The authors.

The N_{60} and Vs are plotted together with the correlations of other authors in Fig. 8, where it is observed that the curves present almost the same trend and are close to each other, possibly because N is corrected at 60% of energy in all cases, regardless of the SPT procedure and equipment. The correlation curve proposed in this publication ($V_S = 141.14\ N_{60}^{0.212}$) is close to that of [9], who used an energy ratio of 75%, close to the one used in this publication (Er = 70%).

3.3 Correlation equation considering the effective overload correction

It is known that Vs and N are corrected differently to the effective stress Eq. (5, 6) and it is expected that these differences introduce a fit trend in the model.

$$(N_1)_{60} = \left(\frac{P_a}{\sigma_v'}\right)^n \cdot N_{60} \quad (5)$$

$$V_{s1} = \left(\frac{P_a}{\sigma_v'}\right)^m \cdot V_s \quad (6)$$

Where: σ_v' is the effective overload stress, Pa is the admospheric pressure and values of n and m are the differences in the way that Vs and N_{60} are corrected for effective overload. Replacing $(N_1)_{60}$ and V_{S1} in the potential equation Eq. (7), Then expressing in terms of natural logarithms and ordering, the linear equation Eq. (9) in two variables is obtained ($\ln N_{60}$ and $\ln \frac{P_a}{\sigma_v'}$):

$$V_{s1} = \left(\frac{P_a}{\sigma_v'}\right)^m \cdot V_s \qquad (N_1)_{60} = \left(\frac{P_a}{\sigma_v'}\right)^n \cdot N_{60} \quad (7)$$

$$Vs = A\,N^B$$

$$\left(\frac{P_a}{\sigma_v'}\right)^m x\, V_S = A\ x\ \left[\left(\frac{P_a}{\sigma_v'}\right)^n x\ N_{60}\right]^B \quad (8)$$

$$\ln V_S = \beta_0 + \beta_1 \ln N_{60} + \beta_2 \ln\left(\frac{P_a}{\sigma_v'}\right) + \varepsilon \quad (9)$$

Where: $\beta_0 = \ln A$; $\beta_1 = B$; $\beta_2 = n*\beta_1 - m$, and ε is the random error term that is normally distributed with zero mean. Table 3 shows the values of β that were determined by the multiple linear regression analysis method and then Eq. (10) is obtained.

$$V_S = 168.35\ (N_{60})^{0.163} \quad (10)$$

[11,13] worked the correlation of N_{60} -Vs, incorporating the influence of the effective overload and applying a multiple linear regression analysis to obtain the correlation. In Fig. 9, the proposed curve in this publication ($V_S=168.35N_{60}^{0.163}$) is slightly close to that of [11] and diverges from [13]. The differences would be associated with the geological nature of the soil. For example, the work in this presentation is on sand from an eolian deposit, and [13] on sands of an alluvial deposit in Mashhad, Iran.

3.4 Model Validation

Geotechnical engineering by its nature requires tools to deal with large uncertainties and variations in material properties [42]. To validate the multiple linear regression model, it is important to evaluate the data spread and the residual analysis.

3.4.1 Data dispersion

The dependent variable ln(Vs) and any of the regressor variables $\ln(N_{60})$ and $\ln(Pa/\sigma_v')$ are expected to have an almost linear relationship. Fig. 10 shows the dispersion of data with a linear trend between the variable ln(Vs) and the regressor variables $\ln(N_{60})$ and $\ln(Pa/\sigma'_v)$, therefore, the adjustment to a multiple linear regression model is valid.

Table 3.
Regression constant and standard deviation of the error.

Soil	$\beta_0 = \ln A$	$\beta_1 = B$	$\beta_2 = n*\beta_1 - m$	ε
Sands	5.1261	0.1634	-0.0827	0.110

Source: The authors.

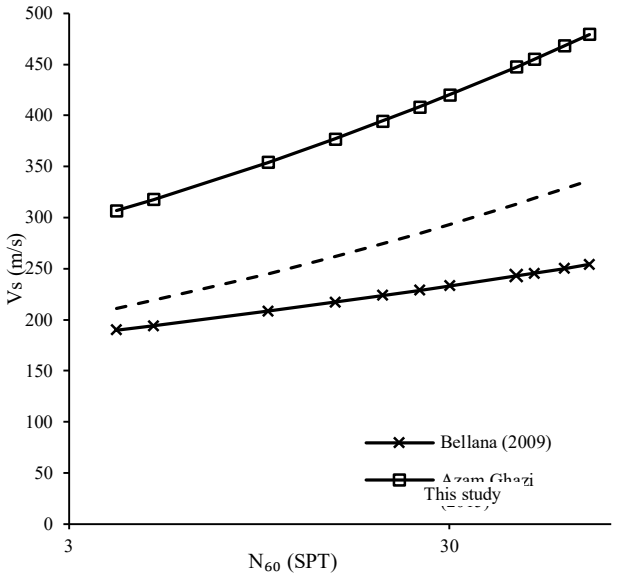

Figure 9. Correlation of N_{60} – Vs, with effective overload influence.
Source: The authors.

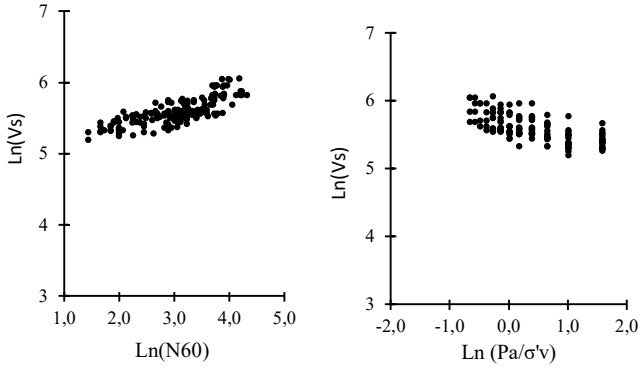

Figure 10. $\ln(V_S)$ Versus $\ln(N_{60})$ and $\ln(P_a/\sigma'_V)$ for sands.
Source: The authors.

According to the data dispersion, Vs would be more related to N than to (Pa/σv') in the range of engineering interest for sands. Vs has a relative influence of (Pa/σv') and carelessness would introduce a trend in the results. This finding is significant since the effect of overload has not been directly quantified in most previous studies.

One of the hypotheses of the multiple linear regression model is that the regressor variables ($\ln(N_{60})$ and $\ln(P_a/\sigma'_V)$ must not have a linearity relationship (in other words, it establishes that there must not be perfect multicollinearity on the model). If the regressive variables show a trend of linear relationship, then there are multicollinearity problems [5]. In Fig. 11 it is observed that the regressor variables do not present a linear relationship.

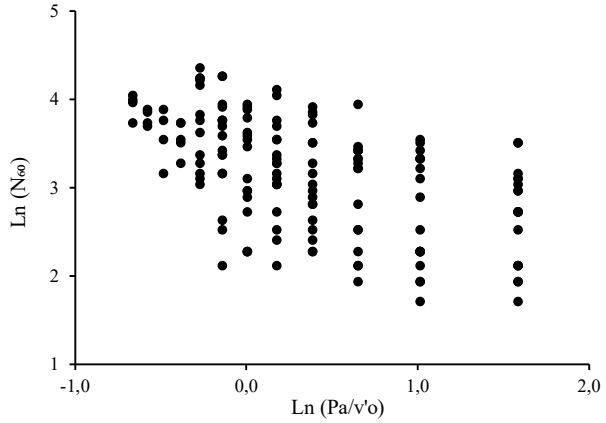

Figure 11. Data dispersion between regressor variables.
Source: The authors.

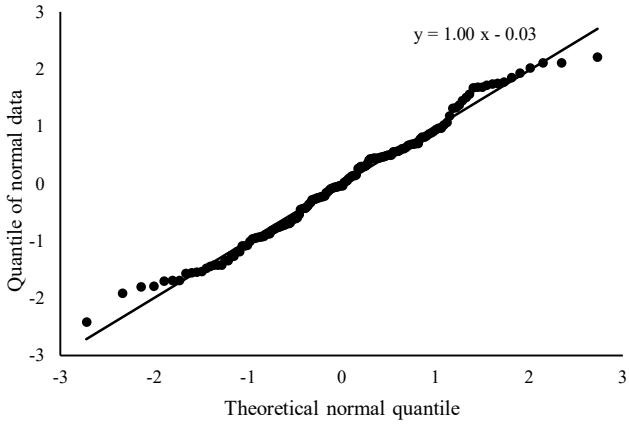

Figure 13. Q-Q plot of the model residuals.
Source: The authors.

The variance influence factor (VIF) also checks for multicollinearity problems in a regression model. According to the VIF, it was verified that there are no multicollinearity problems in the regressor variables since the VIF=1/(1 − $R^2_{ajusted}$) is 2.96, less than 10 ($R^2_{ajusted}$ is 0.666).

3.4.2 Residual Analysis

The fundamental hypothesis of the multiple linear regression model is that the residuals have a zero mean and have a normal distribution. The model residuals, defined as $\ln(V_S) - [\beta_0 + \beta_1 \ln(N_{60}) + \beta_2 \ln(P_a/\sigma'_V)]$ are plotted against the variables $\ln(N_{60})$ and $\ln(P_a/\sigma'_V)$ *in* Fig. 12, and it is observed in both graphs that the mean value of the residuals is zero and they do not present a trend or bias with respect to $\ln(N_{60})$ and $\ln(P_a/\sigma'_V)$, which indicates that the regression has eliminated the trend with respect those input variables (explanatory variables of the regression model).

The residues present a normal distribution with a diagonal straight-line trend in the quantile – quantile (Q - Q) graph. Fig. 13 shows some deviations in the extremes that could be associated with the sampling variability since the data in the tails are often not well sampled and are generally called atypical points.

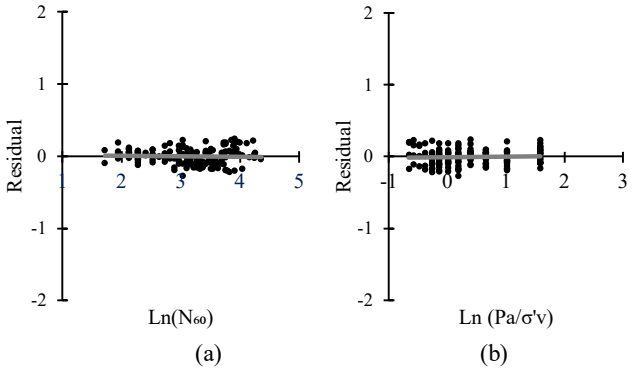

Figure 12. Residuals of the multiple linear regression model for sands. (a) residual versus $\ln(N_{60})$. (b) Residual versus $\ln(P_a/\sigma'_V)$.
Source: The authors.

4. Conclusions

Eq. (11) is the correlation N_{60} - Vs. Eq. (12) is the correlation of N_{60}-Vs, including the effective overload correction to Vs and N_{60}, the latter was determined with a multiple linear regression model. The hypothesis of the model was verified in Item 3.4:

- In the data dispersion, the dependent variable presents a linear or almost linear relationship with each of the regressor variables and the regressor variables do not present a linear relationship.
- In the residual analysis, these have a zero mean and present a normal distribution in the quantile-quantile (Q-Q) graph.

$$V_S = 141.14\ (N_{60})^{0.212} \qquad (R^2_{ajusted} = 0.62) \qquad (11)$$

$$V_S = 168.35(N_{60})^{0.163} \qquad (R^2_{ajusted} = 0.67) \qquad (12)$$

The correlations proposed in this publication are intended to be used to obtain a preliminary estimate of N or Vs where they are not available, and will not be used as a substitute for field measurements, as they may contain considerable uncertainties. The geological conditions of the study area make the correlation proposed in this publication applicable in eolian sand deposits.

References

[1] Nazarian, S.K., Stokoe-II, K. and Hudson, W.R., Use of spectral analysis of surface waves method for determination of moduli and thicknesses of pavement systems, Transportation Research Record 930, pp. 38-45, 1983.

[2] Stokoe, K.H. and Nazarian S.K. Use of rayleigh waves in liquefaction studies, In Woods, R.D., ed., Proc., Measurement and Use of Shear Wave Velocity for Evaluating Dynamic Soil Properties, Colorado, ASCE, New York, USA, 1985, pp. 1-17.

[3] Park, C.B., Miller, R.D. and Xia, J., Multichannel analysis of surface waves. Geophysics-Wisconsin then Tulsa- Society of Exploration Geophysicists, 64(3), pp 800-808, 1999. DOI: 10.1190/1.1444590.

[4] Tokimatsu, K., Geotechnical site characterization using surface waves. International Conference on Earthquake Geotechnical Engineering, 3, Tokyo, 1997. pp. 1333-1368.

[5] Montgomery, D., Peck, E.A. y Vining, G., Introducción al análisis de regresión lineal, Continental, Ciudad de México, Mexico, 2005.

[6] Palacios, O. and De la Cruz, N., Mapa geológico de los cuadrángulos de Las Salinas y Mórrope. Instituto Geológico, Minero y Metalúrgico (INGEMET),

Perú, [en línea]. 1980. Disponible en: http://repositorio.ingemmet.gob.pe/handle/ingemmet/151.
[7] Norma Técnica E.030. Diseño sismorresistente. Reglamento Nacional de Construcciones, Perú, 2018.
[8] Dickenson, S.,E. Dynamic Response of soft and deep cohesive soils during the Loma Prieta Earthquake of October 17th of 1989. PhD Thesis. Dept. of Civil and Enviro. Eng., University of California, Berkeley, CA, USSA, 1994.
[9] Pitilakis K., Raptakis D., Lontzetidis K., Tika-Vassilikou T. and Jongmans D., Geotechnical and geophysical description of Euro-Seistests, using field and laboratory tests and moderate strong motion recordings. Journal of Earthquake Engineering, 3(3), pp 381-409, 1999. DOI: 10.1080/13632469909350352.
[10] Hasancebi, N. and Ulusay, R., Empirical correlactions between shear wave velocity and penetration resistance for ground shaking assessments. Bull Eng Geol Environ, 66(2), pp 203-213, 2007. DOI: 10.1007/s10064-006-0063-0.
[11] Bellana, N., Shear wave velocity as function of SPT penetración resistance and vertical effective stress at California Bridges sites. Msc. Thesis, Department of Civil Engineering, Universidad de California, Los Ángeles, USA, 2009.
[12] Maheswari, R.U., Boominathan, A. and Dodagoudar, G.R., Use of surface wave in statistical correlations of shear wave velocity and penetration resistance of Chennai soils. Geotech Geol Eng, 28(6), pp 119-137, 2010. DOI: 10.1007/s10706-010-9334-4.
[13] Ghazi, A., Moghadas, N.H., Sadeghi, H., Ghafoori, M. and Lashkaripur, G.R., Empirical relationships of shear wave velocity, SPT_N value and vertical effective stress for different soils in Mashhad, Iran. Annals of Geophysics, 58(3), pp. 1-13, 2015. DOI: 10.4401/ag-6635.
[14] Tsai, C.C., Kishida, T., Kuo, C.H., Unified correlation between SPT-N and shear wave velocity for a wide range of soil types considering strain-dependent behavior. Journal Soil Dynamics and earthquake engineering, 126, art. 105783, 2019. DOI: 10.1016/j.soildyn.2019.105783.
[15] Kanai, K., Conference on Cone Penetrometer. The Ministry of Public Works and Settlement. Ankara, Turkey, 1966.
[16] Shibata, T., Analysis of liquefaction of saturated sand during cyclic loading. Disaster Prevention Res. Inst. Bull. 13, pp. 563-570, 1970. DOI: 10.3208/sandf1960.12.1
[17] Ohba, S. and Toriumi, I., Dynamic response characteristics of Osaka Plain. Proceedings of the Annual Meeting, A.I.J., Japan, 1970.
[18] Ohsaki, Y. and Iwasaki, R., On dynamic shear moduli and Poisson's ratio of soil deposits. Soil Found 13, pp. 61-73, 1973. DOI: 10.1016/0148-9062(74)91792-6.
[19] Ohta, T., Hara, A., Niwa, M. and Sakano, T., Elastic shear moduli as estimated from N-value. Proc. 7th Ann. Convention of Japan Society of Soil Mechanics and Foundation Engineering, 1972, pp. 265-268.
[20] Imai, T., P and S wave velocities of the ground in Japan. Proceeding of IX International Conference on Soil Mechanics and Foundation Engineering, 1977, pp. 127-132.
[21] Ohta, Y. and Goto, N., Empirical shear wave velocity equations in terms of characteristics soil indexes. Earthquake Engineering and Structural Dynamics 6, pp. 167-187, 1978. DOI: 10.1016/0148-9062(79)90066-4.
[22] Imai, T. and Tonouchi, K., Correlation of N-value with S-wave velocity and shear modulus. Proceedings of the 2nd European Symposium of Penetration Testing, Amsterdam, Netherlands, 1982. pp. 57-72.
[23] Sykora, D.E. and Stokoe, K.H., Correlations of in situ measurements in sands of shear wave velocity. Soil Dynamics and Earthquake Engineering 20, pp. 125-136, 1983.
[24] Lee, S.H., Regression models of shear wave velocities. Journal of the Chinese Institute of Engineers 13, pp. 519-532, 1990. DOI: 10.1080/02533839.1990.9677284.
[25] Raptakis, D.G., Anastasiadis, S.A.J., Pitilakis, K.D. and Lontzetidis, K.S., Shear wave velocities and damping of Greek natural soils. 10th European Conference on Earthquake Engineering, Vienna, Austria, 1995, pp. 477-482.
[26] Hasançebi, N. and Ulusay, R., Empirical correlations between shear wave velocity and penetration resistance for ground shaking assessments. Bulletin of Engineering Geology and the Environment 66, pp. 203-213, 2007. DOI: 10.1007/s10064-006-0063-0.
[27] Hanumantharao, C. and Ramana, G.V., Dynamic soil properties for microzonation of Delhi, India. Journal of Earth Systen Science 117(S2), pp. 719-730, 2008. DOI: 10.1007/s12040-008-0066-2.
[28] Dikmen, U., Statistical correlations of shear wave velocity and penetration resistance for soils. Journal of Geophysics and Engineering 6, pp. 61-72, 2009. DOI: 10.1088/1742-2132/6/1/007.
[29] Anbazhagan, P., Parihar, A. and Rashmi H.N., Review of correlations between SPT N and shear modulus: a new correlation applicable to any region. Soil Dynamics and Earthquake Engineering, 36, pp. 52-69, 2012. DOI: 10.1016/j.soildyn.2012.01.005
[30] Esfehanizadeh M, Nabizadeh F and Yazarloo, R., Correlation between standard penetration and shear wave velocity for young coastal sands of the Caspian Sea. Arabian Journal of Geosciences 8, pp. 7333-7341, 2015. DOI: 10.1007/s12517-014-1751-x.
[31] Fatehnia M., Hayden M. and Landschoot, M., Correlation between shear wave velocity and SPT-N values for North Florida soils. Elec. J. Geotech. Eng., 20, pp. 12421-12430, 2015.
[32] Kirar, B., Maheshwari, B.K. and Muley, P., Correlation between shear wave velocity (Vs) and SPT Resistance (N) for Roorkee Region. International Journal of Geosynthetics and Ground Engineering, 2, art. 9, 2016. DOI: 10.1007/s40891-016-0047-5.
[33] Rocha, B.P. and Giacheti, H.L., Site characterization of a tropical soil by in situ tests. DYNA, 85(206), pp. 211-219, 2017. DOI: 10.15446/dyna.v85n206.67891.
[34] Kovacs, W. and Salomone, L., SPT hammer energy measurement, ASCE, Vol. 108(4), pp. 599-621, 1982. DOI: 10.1061/AJGEB6.0001278.
[35] Atala, A.C., Estudio experimental sobre correlaciones en suelos granulares finos (arenas) compactados, usando equipos de penetración, Msc. Thesis, Departamento de Geotecnia, Universidad Nacional de Ingeniería, Lima, Peru, 2011.
[36] Zapata, G.J. and Esquivel, E.R., Evaluation of internal and external stresses on the SPT sampler. DYNA 83(195), pp. 229-236, 2015. DOI: 10.15446/dyna.v83n195.50833.
[37] Skempton, A.W., Standard penetration test procedures and the effects in sands of overburden pressure, relative density, particle size, ageing and overconsolidation. Geothecnique 36(3), pp. 425-447, 1986. DOI: 10.1016/0148-9062(87)91274-5.
[38] Robertson, P.K. and Wride, C.E., Evaluating cyclic liquefaction potential using the cone penetration test. Canadian Goetechnical Journal, Ottawa, 35(3), pp 442-459, 1998. DOI: 10.1139/t99-101.
[39] Youd, T.L. et al., Liquefaction resistance of soils: summary report from the 1996 NCEER and 1998 NCEER/NSF workshops on evaluation of liquefaction resistance of soils. Journal of Geotechnical and Geoenvironmental Engineering, 127, pp 817-833, 2001. DOI: 10.1061/(ASCE)1090-0241(2001)127:4(297).
[40] Zeng, C., Xia J.H., Miller, R.D. and Tsoflias, G.P., An improved vacuum formulation for 2D finite-difference modeling of Rayleigh waves including surface topography and internal discontinuities. Society of Exploration Geophysicists, 77, pp. T1-T9, 2012. DOI: 10.1190/GEO2011-0067.1.
[41] Park, C.B., Miller, R.D. and Xia, J., Imaging dispersion curves of surface waves on multichannel record. In: SEG Expanded Abstracts, 1998, pp. 1377-1380. DOI: 10.1190/1.1820161.
[42] Sanchez, A.L. and Ramirez, B.G., Implementation of the confidence interval approach as geostatistical nonlinear modeling for space geotechnical variables. DYNA, 79(173), pp. 15-24, 2012.

C.G. Alhuay-Leon, is a BSc. Eng. Civil Engineering in 2013, from the National University of Engineering (UNI), Peru. Currently a MSc. student in Geotechnical Engineering in the National University of Engineering, Peru. He has experience in the geotechnical engineering area, acting mainly on the following themes: soil investigation, foundations, and excavations, slope stability. Nowadays, Mr. Alhuay is Head of Department of Geotechnical Engineering of Company Sotelo & Asociados, Perú.
ORCID: 0000-0003-2239-2140

P.C. Trejo-Noreña, is BSc. Eng. in Civil Engineering in 2007, from the Engineering National University, Peru. He completed a MSc. in Geotechnical Engineering in 2012, from the University of São Paulo, Brazil, and has obtained his PhD in Geotechnical Engineering in 2015, in the Graduate School in Research and Engineering from the Federal University of Rio do Janeiro COPPE/UFRJ, Brazil. Currently, works at the Postgraduate Department of Civil Engineering at the National University of Engineering, Lima Peru. Mr. Trejo does research in geotechnical engineering: geotechnical instrumentation, foundations, rock mechanics, and He has been working with in situ and laboratory tests for site characterization of soils. Also, Mr. Trejo is Head of Department of Geotechnical Engineering of Company PTN Consultores, Perú.
ORCID: 0000-0001-5225-7340